Minijets, QCD, and Unitarity

A. Capella and J. Tran Thanh Van
Laboratoire de Physique Théorique et Hautes Energies, Université de Paris XI, 91405 Orsay, France

and

J. Kwiecinski
Department of Theoretical Physics, Institute of Nuclear Physics, 31-342 Krakow 23, Poland
(Received 29 December 1986)

We introduce the minijet cross section, computed from QCD, together with a standard soft component, into a unitarization scheme (eikonal model) and show that most of the increase of the inelastic cross section between CERN ISR and SPS collider energies is due to the soft component. We also show that the main properties of minijet production, observed by the UA1 collaboration, can be understood by the introduction of semihard scattering in the dual parton model.

PACS numbers: 13.87.Ce, 12.38.Bx, 12.40.Pp, 13.85.−t

The study of semihard events (minijets) in high-energy hadronic interactions is a fascinating subject that has recently received considerable attention both experimentally[1] and theoretically.[2,3] The interesting minijet analysis performed by the UA1 collaboration, when repeated at higher energies, will offer the opportunity to test QCD in the $x \to 0$ limit. At present energies, it is already quite interesting to compare the measured minijet cross section with standard perturbative QCD calculations. Moreover, the UA1 results raise a lot of challenging questions: Can the semihard-scattering contribution account for the increase with energy of the total cross section? Why is the average multiplicity of the minijet events twice as large as the no-jet one? What is the effect of minijet events in the multiplicity distributions? Why is the correlation between $\langle p_T \rangle$ and multiplicity so different in the minijet and no-jet event samples?

Minijet cross sections and QCD.—The dominant part of the minijet cross section is expected to come from semihard processes, where transverse momenta are relatively large (say $p_T \geq 2$ GeV) and interactions of partons carrying very small longitudinal momentum fractions ($x \leq 10^{-1}$) are involved. In these regions, gluons are expected to play the predominant role and the corresponding integrated inclusive gluon jet cross section $\sigma_{\rm jet}$ can be computed by conventional QCD-improved parton-model formulas.[4] The cross section is already in the millibarn range at CERN SPS collider energies[5,6] and reaches a value close to 200 mb at Superconducting Super Collider energies.[5] This strong increase of $\sigma_{\rm jet}$ is linked with the increase of the gluon distribution function (multiplied by x) at $x \to 0$, which is a straightforward consequence of perturbative QCD.[7,8] However, it should be noticed that $\sigma_{\rm jet}$ is an inclusive cross section which measures (by definition) the average number of semihard interactions multiplied by the inelastic cross section. Therefore, it cannot be identified with the inelastic cross section of minijet events (which will be denoted by σ_H), unless only one semihard interaction can take place. This is not the case at small x. Indeed, in this case, one has to treat on the same footing[8,9] the powers of $\ln(1/x)$ and the power of $\ln(p_T^2)$ appearing in the evolution equations defining gluon distributions. By our doing so, the transverse momenta are no longer strongly ordered and thereby the possibility of several semihard interactions is introduced.

An approximate way of taking into account the above effect was presented in Ref. 3, using the partonic picture of the ladder diagrams. The resulting values of σ_H, corresponding to $(p_T^2)^{\rm min} = 5$ GeV^2, can be parametrized as follows:

$$\sigma_H = 0.10(s - 2450)^{0.35}, \qquad (1)$$

where σ_H is in millibarns and s in square gigaelectronvolts. This parametrization is very good up to $\sqrt{s} = 2$ TeV. (In the numerical calculations it will only be used in this energy range.) At $\sqrt{s} = 40$ TeV the computed value[3] is $\sigma_H = 122$ mb, substantially smaller than the value $\sigma_{\rm jet}$ obtained in the leading-$\ln(p_T^2)$ calculation. At SPS collider energies, the value of σ_H given by Eq. (1) coincides (within 20%) with the corresponding value of $\sigma_{\rm jet}$ obtained in the leading-$\ln(p_T^2)$ calculation.

Let us now compare Eq. (1) with the minijet cross section measured by the UA1 collaboration. Here $E_T^{\rm min} \geq 5$ GeV,[1] and the corresponding $p_T^{\rm min}$ estimated by the UA1 collaboration is $p_T^{\rm min} \simeq 3$ GeV (4 GeV) at 900 GeV (200 GeV). With these values of the p_T cut one gets[10] $\sigma_H \sim 1.3$ mb at 200 GeV and $\sigma_H \simeq 6$ mb at 900 GeV to be compared with the experimental values of 4 and 18 mb, respectively. We conclude that the QCD calculation reproduces quite well the s dependence of the UA1 data but is too small in absolute value by a factor of 3.[11] This difference is not significant since there is an uncertainty of a factor of 2 in the UA1 data due to systematics.[1]

Minijet cross section and unitarity.— The expression for σ_H in Eq. (1) violates unitarity at very high energies, and therefore has to be incorporated into a unitarization scheme. In order to perform the calculations, we proceed in the framework of the eikonal model with three driving terms: a term σ_S representing the contribution of the nondiffractive soft events (bare soft Pomeron), the semihard contribution σ_H (bare hard Pomeron), and a triple-Pomeron term σ_{TP} to take into account diffractive events. The t dependence of the corresponding amplitudes will be assumed to be exponential, with slopes b_S, b_H, and b_{TP}, respectively. The expression for σ_{tot} can then be obtained in a straightforward way. We get[12]

$$\sigma_{\text{tot}} = \sum_{l+m+n\geq 1} I_{l\,m,n}, \tag{2}$$

where

$$I_{l,m,n} = -\frac{8\pi}{l!m!n!}\left(\frac{-\sigma_S}{8\pi b_S}\right)^l \left(\frac{-\sigma_H}{8\pi b_H}\right)^m \left(\frac{+\sigma_{\text{TP}}}{8\pi b_{\text{TP}}}\right)^n \left(\frac{l}{b_S}+\frac{m}{b_H}+\frac{n}{b_{\text{TP}}}\right)^{-1}.$$

The corresponding expressions for the inelastic and diffractive cross sections can be obtained from Eq. (2) by Abramowski-Kuncheli-Gribov (AKG) cutting rules.[8,13] One gets

$$\sigma_{\text{in}} = \sum_{l+m+n\geq 1} 2^{l+m+n-1} I_{l,m,n}, \tag{3}$$

$$\sigma_D = -\sum_{l\geq 0, m\geq 0, n\geq 1} C_n 2^{l+m+n-1} I_{l,m,n}, \tag{4}$$

$$C_n = 2(\tfrac{3}{2})^n - 2.$$

Likewise, the cross section for semihard events after absorption (i.e., the observable one) is given by[14]

$$\sigma_H^{\text{abs}} = \sum_{l=0, m\geq 1, n=0} 2^{l+m+n-1} I_{l,m,n}. \tag{5}$$

We use the parametrization $\sigma_S = as^{\alpha-1}$; for σ_H we take the expression in Eq. (1) (multiplied by a K factor equal to 1.5 in order to normalize it to the experimental data); and σ_{TP} is obtained[15] by integration of the triple-Pomeron formula. For the slopes we take $b_S = b + \alpha' \ln s$, $b_H = b$,[16] and $b_{\text{TP}} = b_S$.[12]

A reasonable fit to the experimental data on σ_{tot}, σ_{in}, and σ_D from middle ISR to top collider energies is obtained with the following values of the parameters: $\alpha = 1.076$, $\alpha' = 0.24$ GeV^{-2}, $a = 37.8$ mb, $b = 3.51$ GeV^{-2}, $c = 40.0$ mb.[15] The results are shown in Fig. 1 and compared with experimental data. The results obtained by putting $\sigma_H = 0$ are also shown. The predictions up to $\sqrt{s} = 40$ TeV are given. We can see in Fig. 1 that the cross section of minijet events σ_H^{abs} is very close to σ_H throughout the collider energy range.[14] However, the contribution to σ_{tot} or σ_{in} of *all* the terms proportional to the semihard interaction driving term σ_H turns out to be much smaller than σ_H^{abs}. As a consequence of this phenomenon, which is quite common in unitarization schemes,[17] a considerable fraction of the rise with energy of σ_{tot} and σ_{in} is due to the soft component.

Minijet production and the dual parton model.— In the case of soft scattering, the dominant diagram in the dual parton model[18] (DPM) (which is the leading order in the $1/N$ expansion and corresponds to a single inelastic collision) contains two chains or strings stretched between valence quarks and diquarks of the colliding hadron. The nonleading diagrams (corresponding to multiple inelastic scattering) contain extra chains involving sea quarks coming mainly from gluon decay (see Fig. 2). The crucial point that we want to make here is that, since the semihard scattering involves a gluon-gluon interaction, *the dominant diagrams are here the four-chain diagrams of Fig. 2,* in which the two gluons in-

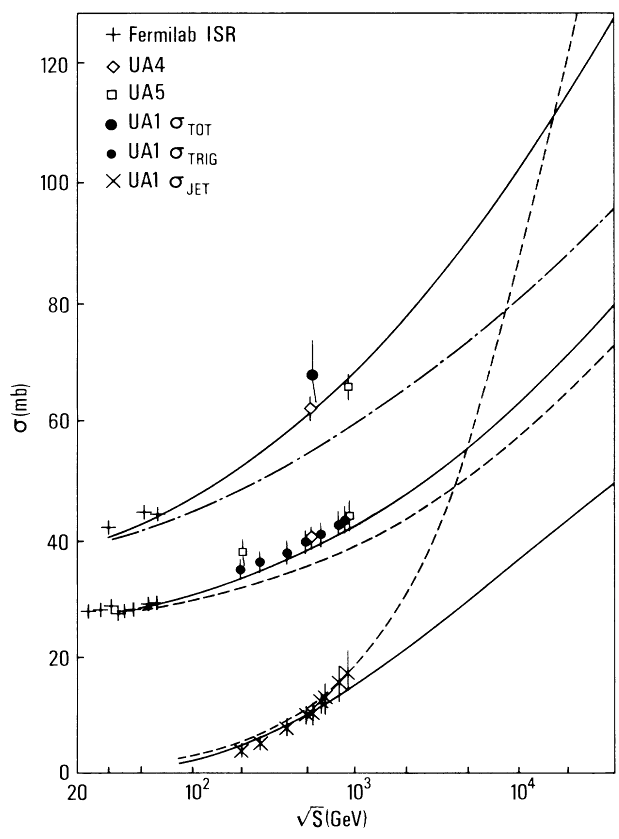

FIG. 1. $\sigma_{\text{tot}}, \sigma_{\text{in}}$ nondiffractive, and minijet cross section σ_H^{abs} (absorbed), computed from Eqs. (2)–(5) (full lines), are compared with the experimental data. The dotted line is the input minijet cross section σ_H and the dashed line (dash-dotted line) is the inelastic nondiffractive cross section (total cross section) obtained with $\sigma_H = 0$.

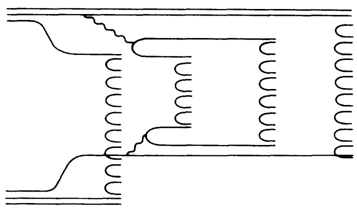

(a)

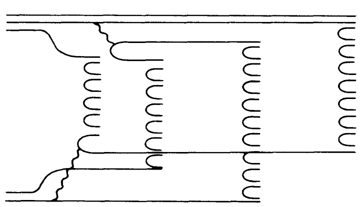

(b)

FIG. 2. Dominant four-chain diagrams for minijet production via a semihard gluon-gluon scattering. The two gluons are represented by wavy lines.

volved have experienced a semihard scattering. This different topology of the dominant diagrams (two chains for no jet, and four chains for jet events) has the obvious consequence that the average multiplicity of the jet-event sample is larger than the no-jet one. This fact has been so far quite puzzling. Indeed, in view of the small values of $p_T^{\min}$ involved in minijet events, one can hardly expect any dramatic differences in the fragmentation of hard and soft initiated strings.[19] In the numerical calculations reported below, we have assumed that these differences are negligible, i.e., we have used the same fragmentation functions for soft and hard chains. The only differences in the average multiplicities will then come from the different topologies mentioned above and from the relative weights σ_k of the various multichain diagrams —which are different for the jet and no-jet event samples. The latter can be obtained by the AKG cutting rules. All the necessary formulas can be found in Ref. 18. (The introduction of the semihard contribution in those formulas is straightforward.) We obtain in the collider energy range $\langle n\rangle_{\rm jet}\sim 1.6\langle n\rangle_{\rm no\,jet}$, to be compared with the experimental result[1] $\langle n\rangle_{\rm jet}\sim 2\langle n\rangle_{\rm no\,jet}$. This difference might be due to different hadronization properties of the soft and hard chains, as discussed above. However, we believe that it is mostly due to the experimental cuts.[20]

We have also computed the changes in the multiplicity distributions due to the introduction of the hard component. The differences with respect to the results obtained in Ref. 18 (without the semihard component) are very small[21] and are hardly noticeable in the figures presented there. Thus the DPM mechanism of Koba-Nielsen-Olesen (KNO) scaling violation (which is due to the growth with energy of the q_s-$\bar{q}_s$ chains) is maintained in the presence of minijet events. The difference between the KNO distributions for the jet and no-jet samples is largely due to the difference in average multiplicity of the two samples and can be qualitatively reproduced in the DPM.

We turn next to the correlation $\langle p_T\rangle$ versus multiplicity. It has been shown[22,23] that a correlation between $\langle p_T\rangle$ and multiplicity (which exhibits the saturation effect observed experimentally[1]) can be obtained in the DPM by introduction of an intrinsic p_T at the end of the chains. The same approach applies, of course, to the no-jet and jet samples. In the jet sample the $\langle p_T\rangle$ resulting from the diagram of Fig. 2 will, of course, be quite large since it contains the semihard scattering. However, when we increase the multiplicity, diagrams with increasing numbers of extra chains will become dominant. Since these extra chains are soft ones (at collider energies multiple hard collisions are negligibly small), the difference between $\langle p_T\rangle_{\rm jet}$ and $\langle p_T\rangle_{\rm no\,jet}$ will decrease with increasing multiplicities. This feature is clearly seen in the UA1 data.

To perform the numerical calculations we use the formalism developed in Ref. 22; we get

$$\langle p_T^2\rangle_n^{\rm no\,jet}=\langle p_T^2\rangle_0+\frac{\langle (z/x)^2N^{q_s\text{-}\bar{q}_s}\rangle_n}{\langle N_{\rm charged}\rangle_n}(n-2)\langle p_T^2\rangle_n^S, \tag{6}$$

$$\langle p_T^2\rangle_n^{\rm jet}=\langle p_T^2\rangle_0+\frac{\langle (z/x)^2N^{q_s\text{-}\bar{q}_s}\rangle_n}{\langle N_{\rm charged}\rangle_n}[(n-4)\langle p_T^2\rangle_n^S+2\langle p_T^2\rangle^H], \tag{7}$$

where

$$\langle p_T^2\rangle_n^S=(1-n^{-1})\langle p_T^2\rangle^S.$$

The left-hand side of (6) and (7) gives the average p_T^2 of the particles produced in a configuration with n chains, measured in the c.m. of the $\bar{p}p$ collision, for the no-jet and jet event samples. $\langle N_{\rm charged}\rangle_n$ is the average charged multiplicity of such a configuration, computed in the DPM.[18] $\langle p_T^2\rangle_0$ is the average p_T^2 of particles produced in a chain, measured in the c.m. of the chain, and $\langle p_T^2\rangle^S$ and $\langle p_T^2\rangle^H$ are the intrinsic p_T^2 of the soft and hard chains. The quantity $\langle (z/x)^2N^{q_s\text{-}\bar{q}_s}\rangle_n$ was computed in Ref. 22 in the framework of the DPM. Its value at $\sqrt{s}=540$ GeV, in the rapidity window $|y|<2.5$, is about 0.2, practically independent of n. Using this value in (6) and (7), together with $\langle p_T\rangle^S=0.75$ GeV and

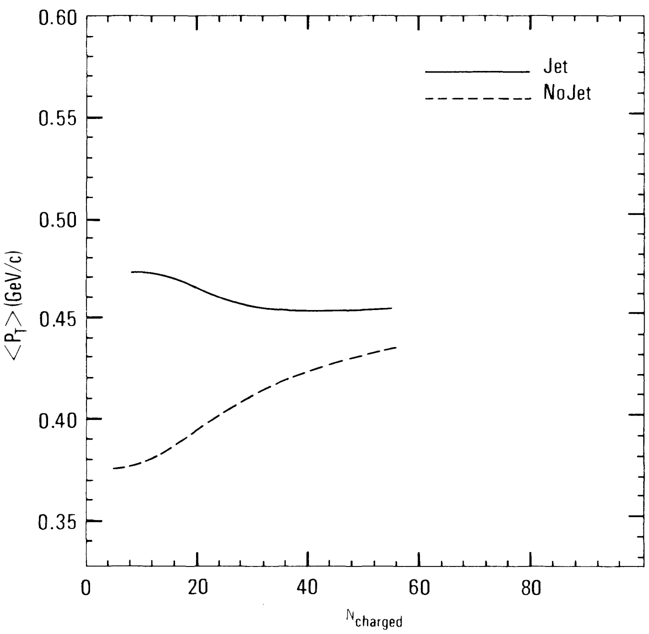

FIG. 3. The correlation of $\langle p_T \rangle$ vs N_{charged} for the jet and no-jet samples at $\sqrt{s}=540$ GeV, and in the rapidity window $|y|<2.5$, computed in the DPM from Eqs. (6) and (7).

$\langle p_T \rangle^H = 1.75$ GeV,[24] we get the results shown in Fig. 3. The correlation $\langle p_T \rangle$ vs N_{charged}, for both the jet and no-jet event samples, reproduces quite well the trend of the UA1 data.[1]

We thank Patrick Aurenche for discussions. One of us (J.K.) would like to thank the Laboratoire de Physique Théorique et Hautes Energies, Orsay, and the Laboratoire de Physique des Particules, Annecy-le-Vieux, for their hospitality. Laboratoire de Physique Théorique et Hautes Energies is a laboratoire associé au Centre National de la Recherche Scientifique.

[1]C. Ciapetti (UA1 Collaboration), in *The Quark Structure of Matter, Proceedings of the Yukon Advanced Study Institute, Yukon, Canada, 1984,* edited by M. Jacob and K. Winter (World Scientific, Singapore, 1986), p. 455; F. Ceradini, in *Proceedings of the International Europhysics Conference on High Energy Physics, Bari, Italy, 1985,* edited by L. Nitti and G. Preparata (European Physical Society, Geneva, 1985), and references therein.

[2]G. Pancheri and C. Rubbia, Nucl. Phys. **A418**, 117 (1984); A. Muller and H. Navelet, Service de Physique Théorique Report No. SPHT/86-094, 1986 (to be published).

[3]J. Kwiecinski, Institute of Nuclear Physics, Cracow, Report No. 1338/PH, 1986 (to be published), and Erratum.

[4]E. Eichten, F. Hinchliffe, K. Lane, and C. Quigg, Rev. Mod. Phys. **56**, 579 (1984).

[5]G. Cohen-Tannoudji, A. Mantrach, H. Navelet, and R. Peschanski, Phys. Rev. D **28**, 1628 (1983); T. V. Gaisser and F. Halzen, Phys. Rev. Lett. **54**, 1754 (1985).

[6]G. Pancheri and Y. Srivastava, Phys. Lett. **159B**, 69 (1985).

[7]Yu. I. Dokshitzer, D. I. Dyakomov, and S. I. Troyan, Phys. Rep. **58**, 269 (1980), and references therein.

[8]L. V. Gribov, E. M. Levin, and M. G. Ryskin, Phys. Rep. **100**, 1 (1983), and references therein.

[9]J. Kwiecinski, Z. Phys. C **29**, 561 (1985).

[10]σ_H decreases approximately as $(p_T^{\min})^{-2}$ when $p_T^{\min}$ is increased.

[11]A similar conclusion is reached in G. Pancheri and Y. N. Srivasta, Laboratori Nazionali di Frascati Report No. 86/31(P), 1986 (to be published).

[12]A. Capella, J. Kaplan, and J. Tran Thanh Van, Nucl. Phys. **B97**, 493 (1975). Phase factors have been rejected.

[13]V. A. Abramowski, V. N. Gribov, and O. V. Kancheli, Yad. Fiz. **18**, 595 (1973) [Sov. J. Nucl. Phys. **18**, 308 (1974)].

[14]σ_H belongs to a class of cross sections which is only self-absorbed. See R. Blankenbecler, A. Capella, J. Tran Thanh Van, C. Pajares, and A. V. Ramallo, Phys. Lett. **107B**, 106 (1981).

[15]The triple-Pomeron formula $d\sigma/dt\,dM^2 = cs^{-1}\exp(bt)(s/M^2)^{1+2\alpha' t}$, integrated over t and M^2 (up to $M^2=s/20$), yields $\sigma_{\text{TP}} = c[\ln(b+2\alpha'\ln(b+2\alpha'\ln 20))]$.

[16]K. Kwiecinski, Z. Phys. C **29**, 147 (1985).

[17]In terms of Reggeon diagrams this phenomenon is due to the (negative) contribution to σ_{tot} of diagrams containing, at the lowest order, one cut soft Pomeron and one uncut hard Pomeron.

[18]A. Capella, A. Staar, and J. Tran Thanh Van, Phys. Rev. D **32**, 2933 (1985), and references therein.

[19]For an opposite point of view see A. D. Martin and C. J. Maxwell, Phys. Lett. **172B**, 248 (1986).

[20]Chao Wei-Gin, Meng Ta-Chung, and Pan Ji-Cai, Frieie Universität, Berlin, Report No. FUB-HEP/86-6, 1986 (to be published).

[21]The introduction of semihard scattering in the DPM has been discussed by P. Aurenche, F. W. Bopp, and J. Ranft [see Siegen University Report No. SI-8-6, 1986 (to be published), and references therein] who reach similar conclusions concerning the source of KNO scaling violation.

[22]A. Capella and A. Krzywicki, Phys. Rev. D **29**, 1007 (1984).

[23]P. Aurenche, F. W. Bopp, and J. Ranft, Phys. Lett. **147B**, 212 (1984).

[24]This value is obtained by our identifying the intrinsic p_T of the hard chains with $p_T^{\min}/2$ (as discussed above, the experimental value of $p_T^{\min}$ is about 3.5 GeV at middle collider energies). We also use $\langle p_T \rangle_0 = 0.37$ GeV, which is the experimental value of $\langle p_T \rangle$ at low multiplicities.